


# The novel sRNA *s015* improves nisin yield by increasing acid tolerance of *Lactococcus lactis* F44

Jiakun Qi<sup>1,2</sup> · Qingge Caiyin<sup>2</sup> · Hao Wu<sup>1,2</sup> · Kairen Tian<sup>1,2</sup> · Binbin Wang<sup>1,2</sup> ·  
Yanni Li<sup>1,2</sup> · Jianjun Qiao<sup>1,2,3</sup> 

Received: 12 April 2017 / Revised: 16 June 2017 / Accepted: 19 June 2017 / Published online: 9 July 2017  
© Springer-Verlag GmbH Germany 2017

**Abstract** Nisin, a polycyclic antibacterial peptide produced by *Lactococcus lactis*, is stable at low pH. Improving the acid tolerance of *L. lactis* could thus enhance nisin yield. Small non-coding RNAs (sRNAs) play essential roles in acid tolerance by regulating their target mRNAs at the post-transcriptional level. In this study, a novel sRNA, *s015*, was identified in *L. lactis* F44 via the use of RNA sequencing, qRT-PCR analysis, and Northern blotting. *s015* improved the acid tolerance of *L. lactis* and boosted nisin yield at low pH. In silico predictions enabled us to construct a library of possible *s015* target mRNAs. Statistical analysis and validation suggested that *s015* contains a highly conserved region (5'-GAAAAAAC-3') that likely encompasses the regulatory core of the sRNA. *atpG*, *busAB*, *cysD*, *ilvB*, *tesR*, *ung*, *yudD*, and *ywdA* were verified as direct targets of *s015*, and the interactions between *s015* and its target genes were elucidated. This work provided new insight into the adaptation mechanism of *L. lactis* under acid stress.

**Keywords** *L. lactis* · Nisin · Acid tolerance · sRNA

J.Q. and Q.C. contributed equally to this work.

**Electronic supplementary material** The online version of this article (doi:10.1007/s00253-017-8399-x) contains supplementary material, which is available to authorized users.

✉ Jianjun Qiao  
jianjunq@tju.edu.cn

<sup>1</sup> Department of Pharmaceutical Engineering, School of Chemical Engineering and Technology, Tianjin University, Tianjin, China

<sup>2</sup> Key Laboratory of Systems Bioengineering, Ministry of Education, Tianjin, China

<sup>3</sup> SynBio Research Platform, Collaborative Innovation Center of Chemical Science and Engineering, Tianjin, China

## Introduction

Bacteria are subjected to various kinds of environmental stresses, including heat/cold shock, oxidative stress, osmotic stress, and low pH conditions (Romeo et al. 2007; Wang et al. 2015, 2016b; Zere et al. 2015). In order to cope with enormous environmental fluctuations, microorganisms have evolved various mechanisms to maintain the intracellular homeostasis. Small non-coding RNAs (sRNAs) play essential roles in regulating the growth and survival via post-transcriptional control of gene expression in both eukaryotic and prokaryotic cells (Wagner and Romby 2015). Furthermore, sRNAs can be induced by environmental changes (Siqueira et al. 2016) and act as crucial regulators for stress responses (Wang et al. 2015, 2016b; Zere et al. 2015) and virulence (Bardill et al. 2011). For example, the sRNAs *ArcZ*, *DsrA*, and *RprA* contribute to acid tolerance in *Escherichia coli*, and *DsrA* and *RprA* are induced under acid stress (Bak et al. 2014). Located between and on the opposite strand of genes encoding two acid response transcriptional regulators called *gadX* and *gadW*, the sRNA *gadY* can form base pairs with the 3'-untranslated region of the *gadX* mRNA, thereby conferring increased stability and allowing for accumulation of *gadX* mRNA and increased expression of downstream acid resistance genes (Opdyke et al. 2004). Additionally, in *Synechocystis*, the expression of the sRNA *NsiR4* was induced by nitrogen limitation (Klahn et al. 2015), as was *NrsZ* (nitrogen-regulated sRNA) (Wenner et al. 2014).

Although small non-coding RNAs represent a very recent discovery, examples of sRNAs in Gram-positive bacteria are still plentiful. In *Lactococcus lactis* MG1363, a recently published transcriptome landscape revealed novel hypothetical small regulatory RNAs involved in carbon uptake and metabolism. Although analysis indicated some previously undescribed small RNAs that could have a

regulatory role in low pH conditions, their specific roles and regulatory mechanisms have not been corroborated (van der Meulen et al. 2016).

In Gram-positive bacteria, sRNAs are known to hybridize with the target mRNAs to inhibit or promote the translation process. The most common sRNAs are trans-encoded sRNAs, which can regulate translation initiation, RNA stability, or protein activity by forming short segments of partial nucleotide complementarity with their target genes. Translation initiation can be inhibited by several different mechanisms depending on the specific location that (a) sRNA pairs directly with the ribosome-binding site (RBS) locus to block the initiation of translation, (b) sRNA induces secondary structural changes in the RBS locus that unfold translation-inhibitory structures or hide the RBS, or (c) sRNA targets downstream of the first five codons in an area where mRNAs are generally sensitive to the antisense inhibition of translation initiation (Storz et al. 2011). Trans-encoded sRNAs have many different target mRNAs, and there is evidence that sRNA-mediated control of translation is prominent in bacteria (Boisset et al. 2007; Chunhua et al. 2012; Huntzinger et al. 2005; Morfeldt et al. 1995).

Some sRNAs are remarkably conserved, indicating that they serve critical cellular functions (Updegrove et al. 2015). In *Salmonella*, one example is SdsR, which is transcribed by the general stress  $\sigma$ -factor and employs two different regions to interact with individual targets (Frohlich et al. 2016). In *Pseudomonas aeruginosa*, the sRNA RgsA, which can regulate the mRNA of the global transcriptional regulator Fis and the acyl carrier protein AccP, also possesses a conserved region that acts as a regulatory core of the sRNA (Lu et al. 2016).

As an antimicrobial peptide with 34 residues, nisin is known to show a broad spectrum of antimicrobial activity against gram-positive bacteria as well as gram-negative bacteria (Rayman et al. 1981; Stevens et al. 1991; Xuanyuan et al. 2010). Previous studies have suggested that nisin could show a relatively higher stability and activity in the environment with lower pH value (Zhang et al. 2014). Improving acid tolerance of *L. lactis* F44 could hence enhance nisin yield (Zhang, et al. 2016).

In this study, we identified the novel sRNA s015 in *L. lactis*, which was found to be widely conserved across many *L. lactis* strains. We showed that s015 contributed to the growth and survival of *L. lactis* F44 subjected to acid stress. In silico analysis of the direct targets of s015 demonstrated that it interacted with its targets at a specific, conserved site. Furthermore, we verified that sRNA s015 directly bound to its targets *atpG*, *busAB*, *cysD*, *ilvB*, *tcsR*, *ung*, *yudD*, and *ywdA* by an antisense mechanism. This work revealed a new sRNA s015 that contributes to increased acid tolerance in *L. lactis* and could serve as a more general model for sRNA-mediated stress responses.

## Materials and methods

### Bacterial strains and growth conditions

The *L. lactis* F44 (wild type) strain used in this work was derived from *L. lactis* YF11 (Zhang et al. 2014, 2016). YF11 is accessible from the China General Microbiological Culture Collection Center under the accession number CGMCC7.52. *Escherichia coli* BL21 was used for the validation of target genes, and *E. coli* TG1 was used for plasmid construction. *L. lactis* was cultured in seed medium (1.5% yeast extract, 1.5% peptone, 2%  $\text{KH}_2\text{PO}_4$ , 1.5% sucrose, 0.15% NaCl, 0.015%  $\text{MgSO}_4 \cdot 7\text{H}_2\text{O}$ ) at 30 °C. *E. coli* BL21 and TG1 strains were cultured in LB medium (1% tryptone, 0.5% yeast extract, and 1% NaCl) at 37 °C. *Micrococcus flavus* ATCC 10240 was used for nisin titer assay and cultured in LB medium at 37 °C. The plasmids used in this study are shown in Supplementary Table S1.

### RNA extraction and small transcript Northern blots

F44 cells were harvested during mid-log phase ( $\text{OD}_{600}$  3.5–4.0) by centrifugation. Total RNA was extracted using the Trizol (Invitrogen, 15596108) procedure according to the manufacturer's instructions. RNA pellets were dissolved in DEPC- $\text{H}_2\text{O}$ . Northern blotting was performed as described with several modifications (van der Meulen et al. 2016). Briefly, at least 10  $\mu\text{g}$  of total RNA was added to 7  $\mu\text{l}$  RNA loading buffer (Sigma R1386 USA) and heated at 65 °C for 10 min before separation on 15% urea polyacrylamide gels. RNAs were transferred to nylon membranes (Thermo AM10100) and cross-linked at 120 J using a UV cross-linker. Membranes were dried at 80 °C. Pre-hybridization was performed at 42 °C for 30 min. The blots were then hybridized overnight at 42 °C in hybridization buffer (Sigma H7033 USA) containing a single-stranded RNA 5' biotin-labeled probe. s015 sRNA and 5S RNA were detected by 5' end-labeled Nbio s015 (5'-AUGGUUUUCUCGAUUCAUUUUU GUCCUUA-3') and Nbio 5S (5'-GGCCACUCGCCUAUCUCCCA GGGGGCAACC-3'), respectively. The membranes were washed three subsequent times with SSC wash buffers supplemented with 0.1% SDS (2 $\times$ , 0.5 $\times$ , and 0.1 $\times$ , respectively). Finally, the hybridization signals were visualized by BIO-RAD ChemiDoc XRS.

### qRT-PCR

Two micrograms of total RNA extracted from F44 cells as described above was reverse transcribed using the TIANScript RT Kit (TIANGEN) according to the manufacturer's instructions. The resulting cDNAs were stored at -80 °C until qRT-PCR analysis. qRT-PCR was performed with Power SYBR Green PCR Master Mix (Applied

Biosystems). Briefly, a 20  $\mu$ l reaction solution containing 1–1000 ng of cDNA, 1  $\mu$ l each of forward and reverse primers (10 mM) (see Supplementary Table S2 for a list of primers used), 10  $\mu$ l of 2 $\times$  Ultra SYBR Mixture (with ROX), and 3  $\mu$ l of sterile water was analyzed on a LightCycler 480 Real-Time PCR System (Roche, Switzerland) according to the manufacturer's instructions. Reactions were run in triplicate in three independent experiments for each condition. The 16S rRNA gene was used as an internal control to normalize cycle threshold (CT) values. Differences in the relative expression levels were calculated with the  $2^{-\Delta\Delta CT}$  method (Zhang et al. 2016).

### Construction of an sRNA *s015* deletion, complementation, and overexpression strains

The homologous double crossover recombination method was used to construct a *L. lactis* F44 *s015* deletion mutant ( $\Delta s015$ ). A detailed protocol has been published previously (Zhu et al. 2014).

The sRNA expression plasmid pLEB-sRNA was constructed from the pLEB124 plasmid backbone with some modifications. The p45-promoter-MCS-terminator fragments including *EcoRI/BglII* restriction sites were amplified using non-template PCR. The *EcoRI/BglII*-digested PCR fragments were cloned into the *EcoRI/BglII*-digested pLEB124 plasmid. The sRNA sequences were amplified from *L. lactis* F44 and cloned into the sRNA expression vector pLEB-sRNA using the homologous recombination method with EasyGeno Kit (TIANGEN). The overexpression and complementation strains (F44-ps015 and F44-cs015, respectively) were obtained by electroporation (2.45 kV) of the pLEB-sRNA-s015 vector into F44 and F44- $\Delta s015$ , respectively.

The accession number of *s015* is KY985350, and the transcriptome sequencing raw data has been submitted to sequence read archive (SRA): SRP105011-PRJNA383925, SRS2139720-sRNA.

### Acid tolerance assays

The F44, F44- $\Delta s015$ , F44-ps015, and F44-cs015 *L. lactis* strains were incubated for three generations before being used in acid tolerance assays. Bacteria of the youngest generation were grown to early logarithmic phase (OD<sub>600</sub> 5.0–5.5) at 30 °C. Cells were harvested by centrifugation (8000 r/s, 8 min, 4 °C) and re-suspended in the same volume of 0.9% NaCl. Cells were then exposed to tryptone aqueous solution (2% tryptone, 0.5% NaCl) at different pH levels (2.0, 3.0, 4.0, 5.0, or 7.0) for 2 h. After treatment, cells were diluted and plated on seed medium. Colony-forming units (CFUs) before and after stress treatment were determined by counting colonies after 24 h of incubation. The strain survival was calculated as the ratio of the CFU at the different sampling times normalized to the ratio obtained at pH 7.0.

### Cell growth assay and nisin titer

The F44, F44- $\Delta s015$ , F44-ps015, and F44-cs015 *L. lactis* strains were incubated for three generations and cultured in fermentation broth (1.5% peptone, 1.5% yeast extract, 1.5% sucrose, 2.0% KH<sub>2</sub>PO<sub>4</sub>, 0.15% NaCl, 0.3% corn steep liquor, 0.26% cysteine, and 0.015% MgSO<sub>4</sub>·7H<sub>2</sub>O). Optical density (OD) was measured at 600 nm every 2 h with a TU-1810 spectrophotometer to monitor cell growth. The nisin titer assay was performed as described previously (Zhang et al. 2016).

### In silico analysis of RNA structures

The *mfold* web server was used to predict the structures of folded RNAs, including both sRNAs and target mRNAs (Waugh et al. 2002; Zuker 2003; Zuker and Jacobson 1998). Default folding conditions were used except for temperature, which was set to 30 °C.

### sRNA target prediction

Target predictions for *s015* were obtained using three different online programs: sTarPicker (sRNATarBase) (Wang et al. 2016a), CopraRNA (Comparative prediction algorithm for small RNA targets) (Busch et al. 2008; Wright et al. 2014) and Interacting RNA (IntaRNA) (Pain et al. 2015), and Target RNA 2.0 (Kery et al. 2014). These programs are available at <http://ccb.bmi.ac.cn/starpicker/>, <http://rna.informatik.uni-freiburg.de/IntaRNA/Input.jsp>, and <http://cs.wellesley.edu/~btjaden/TargetRNA2/>, respectively.

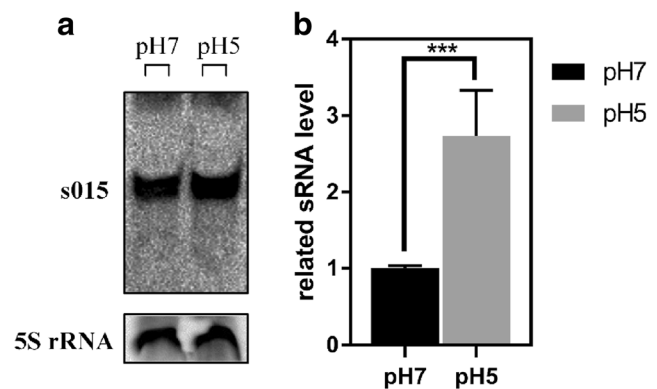


**Fig. 1** **a** Northern blot of *s015* in *L. lactis* F44 at pH 7.0 and pH 5.0. Grayscale analysis indicated a 1.42-fold IOD value (pH 5.0, 31,228.207 vs. pH 7.0, 22,011.945). **b** qRT-PCR of *s015* at pH 7.0 and pH 5.0. Values are normalized to pH 7.0. The error bars represent +1 standard deviation. Statistical differences between each group were analyzed using Student's *t* test; \*\*\**p* < 0.0005

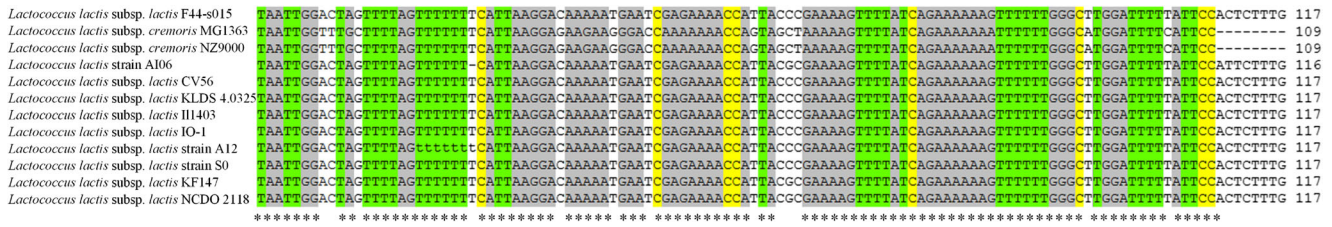


**Fig. 2** *s015* is broadly conserved across *L. lactis* strains. The figure shows alignment of *s015* homologs in related strains. The bases in color are highly conserved

**Validation of sRNA targets using reporter fusion**

Plasmids for these experiments were constructed as described (Urban and Vogel 2007). Briefly, all sRNA plasmids were constructed from the pRSF-Dute-1 plasmid backbone. First, the *s015* sequence and a nonsense control *rrfB* (gi 49175990) sequence were amplified from the *L. lactis* F44 and *E. coli* DH5 $\alpha$  genomes, respectively. *Bam*HI and *Hind*III restriction sites were added to the sequences during amplification. The *Bam*HI/*Hind*III-digested PCR fragments were cloned into the *Bam*HI/*Hind*III-digested pRSF-Dute plasmid. For LacZ-target fragment-eGfp fusion cloning, the pACYC Dute-1 plasmid was used as the backbone. First, the residues spanning codons 2–59 of the *lacZ* gene were amplified. Next, the region spanning from the last 30–40 codons of the upstream C-terminal region to the first 10–15 codons of a potential target gene were fused to the second codon of *eGfp*. Meanwhile, the two fragments above were fused to construct *lacZ*-target fragment-*eGfp*. *Nco*I and *Xho*I restriction sites were added to the fusion DNA fragment, which was then digested and cloned

into the *Nco*I/*Xho*I-digested pACYC plasmid. This plasmid was called pACYC-target (Fig. S1 A). Each pACYC-target plasmid was transformed along with an sRNA plasmid (either *s015* or the nonsense control *rrfB*) into *E. coli* BL21 (Fig. S1 B).

**Results**

**Identification of *s015*, a novel small non-coding RNA upregulated under acid stress**

To study the role of sRNAs in regulating the response to acid stress in *L. lactis* F44, the transcriptome at both pH 5.0 and pH 7.0 was sequenced using the Illumina HiSeq 2000 sequencing platform, and transcript levels were compared between the two conditions (sample SRS2139720—sRNA). The RNA-sequencing results revealed that several sRNAs were upregulated under acid stress, including *s015*, which is located in an intergenic region. To confirm the results of the

**Fig. 3** Effect of *s015* deletion in *L. lactis* F44. **a** The survival rate of *L. lactis* F44, F44- $\Delta$ *s015*, F44-ps*015*, and F44-cs*015* at various pH levels compared to survival rate at pH 7.0. The gray bars indicate fold changes in CFU (calculated as means from acid tolerance experiments) relative to pH 7.0. **b** Growth characteristics of *L. lactis* F44, F44- $\Delta$ *s015*, F44-ps*015*, and F44-cs*015*. **c** Nisin yield of *L. lactis* F44, F44- $\Delta$ *s015*, F44-ps*015*, and F44-cs*015*. **d** The unit nisin production of *L. lactis* F44, F44- $\Delta$ *s015*, F44-ps*015*, and F44-cs*015*

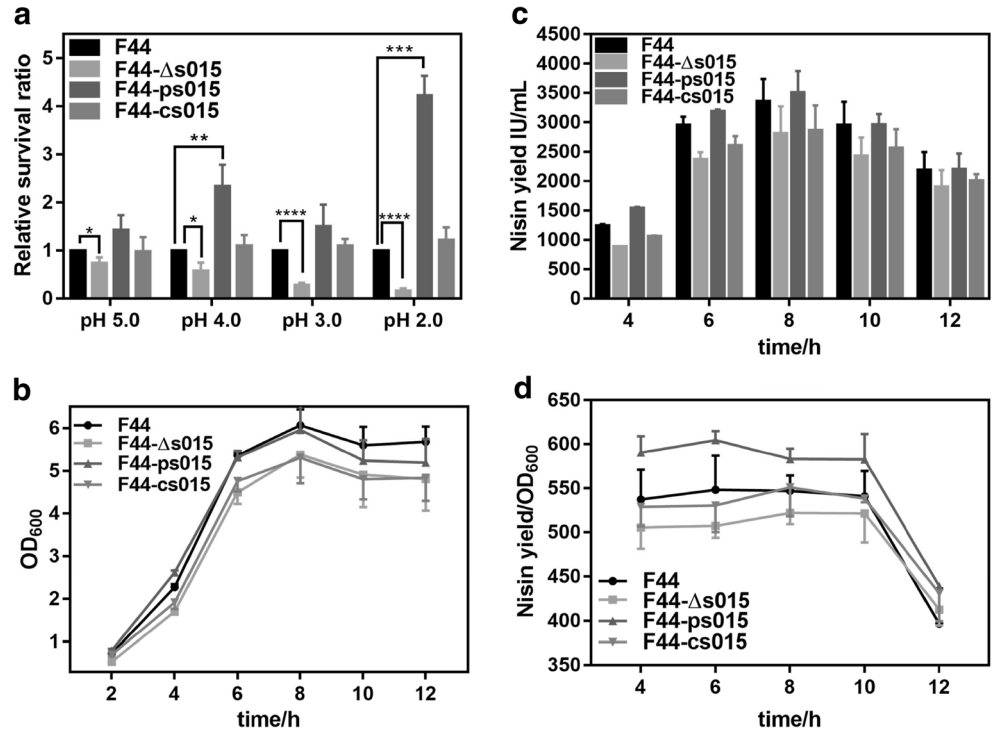


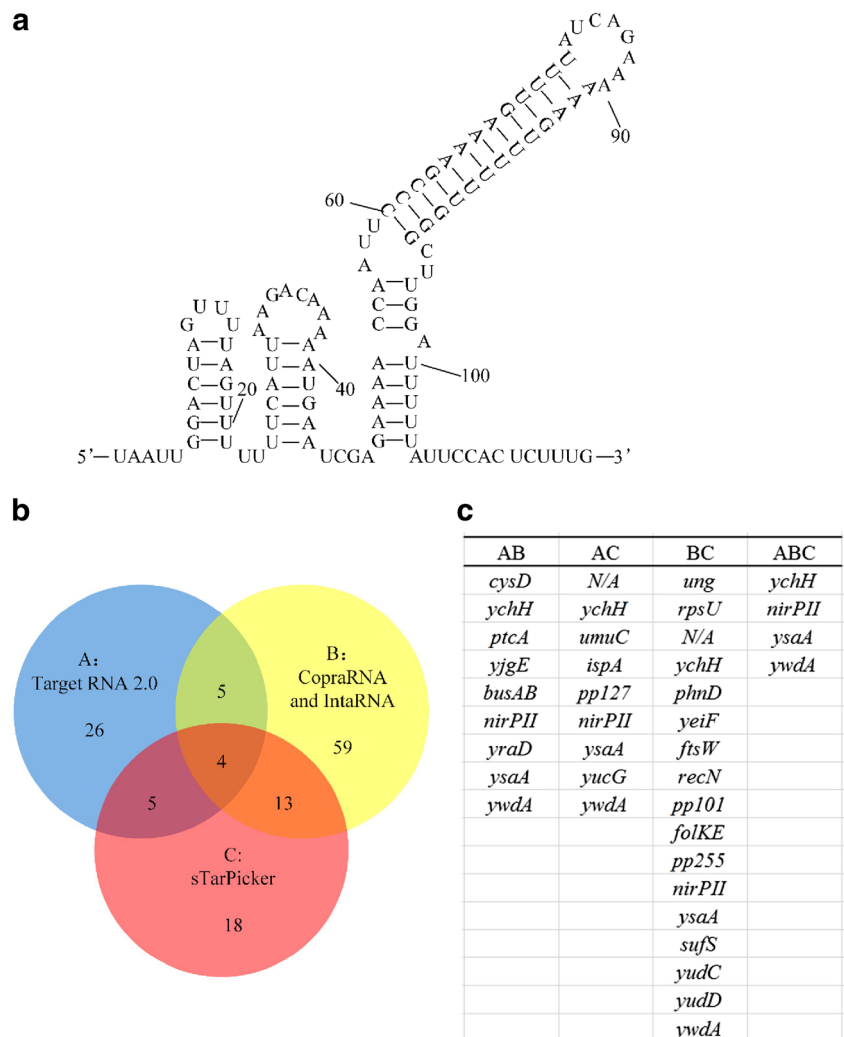
**Table 1** Relative survival ratio of F44- $\Delta s015$ , F44-*ps015*, and F44-*cs015*

	F44- $\Delta s015$	F44- <i>ps015</i>	F44- <i>cs015</i>
pH 5.0	0.738 ± 0.119	1.427 ± 0.309	0.981 ± 0.296
pH 4.0	0.581 ± 0.169	2.334 ± 0.452	1.096 ± 0.227
pH 3.0	0.282 ± 0.048	1.504 ± 0.452	1.102 ± 0.138
pH 2.0	0.162 ± 0.051	4.219 ± 0.416	1.217 ± 0.265

transcriptome sequencing data, we identified sRNA *s015* (KY985350) by Northern blot analysis (Fig. 1a) and qRT-PCR (Fig. 1b), showing that it was upregulated in low pH conditions.

High conservation of *s015* across *L. lactis* strains would suggest an important function in this species. We found that the *s015* gene is indeed conserved in other 11 related *L. lactis* strains, and the most highly conserved regions, namely nucleotides 12–33 and 63–108, are shown in Fig. 2.

**Fig. 4** **a** The secondary structure of *s015* as predicted by *mfold*. **b** Venn diagram showing the overlap among the putative *s015* target genes identified by target RNA 2.0, CopraRNA and IntaRNA, and sTarPicker. **c** The putative target genes identified by one or more prediction programs



### *s015* facilitates *L. lactis* F44 acid tolerance and nisin production

To explore the function of sRNA *s015*, we constructed the *s015* deletion strain F44- $\Delta s015$  as well as an *s015* complemented strain (F44-*cs015*) and an *s015* overexpression strain (F44-*ps015*). As the fermentation process progresses, the bacterial cells suffer increasing levels of acidic stress. In order to evaluate the effects of *s015* under varying degrees of acid stress, *L. lactis* F44, F44- $\Delta s015$ , F44-*ps015*, and F44-*cs015* were exposed to pH conditions ranging from 5.0 to 2.0 for 2 h. Results indicated that the F44- $\Delta s015$  strain displayed a lower survival ratio in acidic conditions compared to the wild type, while the F44-*ps015* strain showed a higher survival ratio. The survival ratio of F44-*cs015* fluctuated around that of the wild-type strain (Fig. 3a and Table 1). We also compared the growth of the four strains in the fermentation broth and found that the wild-type strain grew faster than the F44- $\Delta s015$  strain. However, compared with F44- $\Delta s015$  and *L. lactis* F44, little difference can be observed on the growth of F44-*cs015* and F44-*ps015*,

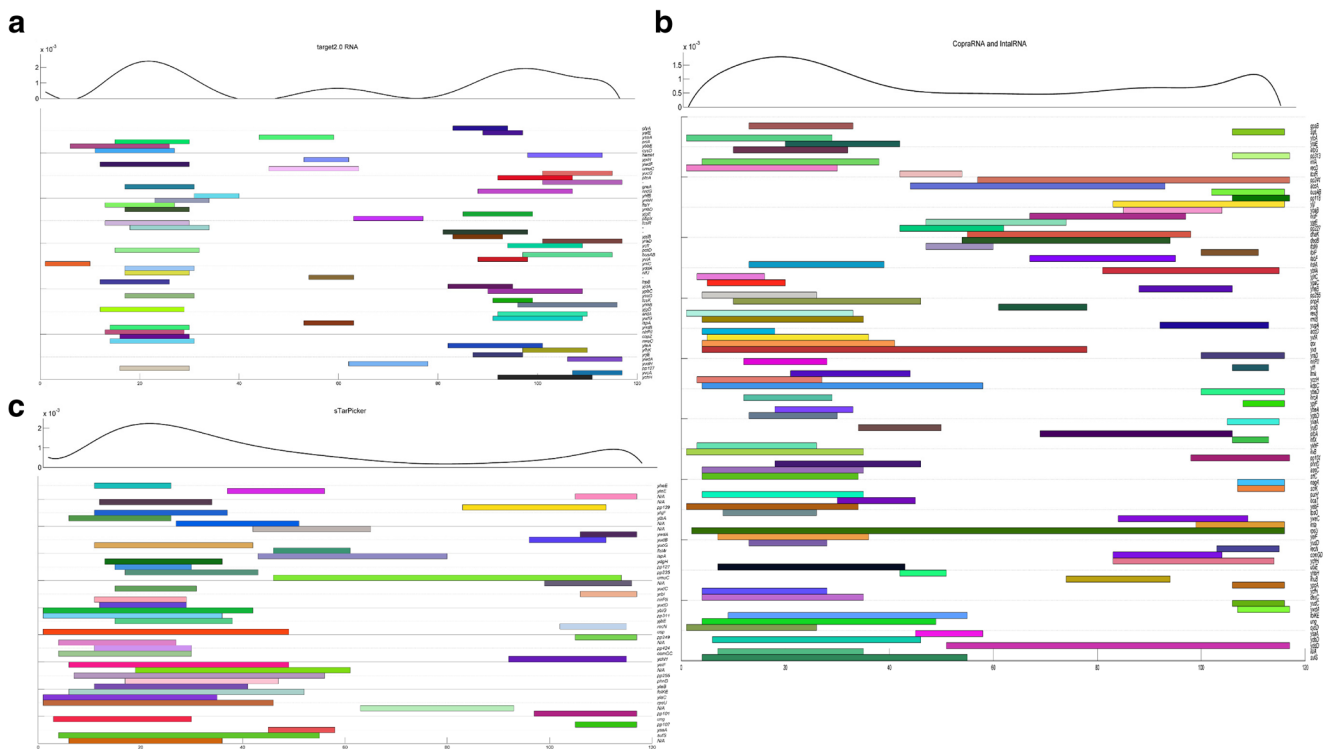


**Fig. 5** The regions binding with targets predicted by **a** target RNA 2.0, **b** CopraRNA and IntaRNA, and **c** sTarPicker. The probability distribution figure shows the probability of s015 binding with target mRNAs. The corresponding targets are listed below

respectively (Fig. 3b). Previous studies have suggested that improving acid tolerance of *L. lactis* F44 could enhance nisin yield (Zhang et al. 2016). Thus, we suspected that the F44- $\Delta$ s015 deletion strain might produce less nisin compared to the wild-type one, as it displays reduced acid tolerance. Accordingly, we hypothesized that F44-ps015 would have improved nisin yields due to its increased acid tolerance and that F44-cs015 would have a similar nisin yield to the wild-type F44. To test this, we measured nisin production using a fermentation assay. As expected, compared to the wild type, the F44- $\Delta$ s015 strain produced less nisin and the F44-ps015 strain had a slightly increased nisin yield. The F44-cs015 strain had a lower nisin yield compared to the wild-type strain (Fig. 3c). Nisin production is generally growth dependent. To account for the impact of biomass on

our results, we calculated the nisin yield per unit biomass. Figure 3d shows that the thus-normalized nisin yield of the F44-ps015 strain is the highest, while that of the F44- $\Delta$ s015 strain is the lowest. No significant difference was observed between the normalized nisin yields of F44 and F44-cs015. Together, these data suggested that s015 plays a crucial role in maintaining the growth of *L. lactis* F44 and improving its nisin yield in acidic conditions.

#### Prediction of target mRNAs of s015 in *L. lactis* F44 via computational analysis

To further characterize sRNA s015 in *L. lactis* F44, the secondary structure of s015 was analyzed using the *mfold* web server

**Table 2** mRNA levels of eight target genes in F44- $\Delta$ s015 compared to F44 as quantified by qRT-PCR

Target gene	Function	qRT-PCR (pH 7)	qRT-PCR (pH 5)
<i>atpG</i>	ATP synthase F1 subunit gamma	1.422 ± 0.090	0.720 ± 0.144
<i>busAB</i>	ABC transporter permease/substrate-binding protein	2.068 ± 0.365	5.172 ± 0.698
<i>cysD</i>	<i>O</i> -Acetyl-L-homoserine sulfhydrylase/ <i>O</i> -acetyl-L-serine sulfhydrylase	0.415 ± 0.135	1.630 ± 0.308
<i>ilvB</i>	Acetolactate synthase large subunit	1.010 ± 0.104	0.466 ± 0.071
<i>tcsR</i>	Two-component response regulator	0.396 ± 0.124	0.494 ± 0.071
<i>ung</i>	Uracil-DNA glycosylase	0.406 ± 0.149	0.519 ± 0.004
<i>yudD</i>	Flavin-nucleotide-binding protein	1.152 ± 0.177	1.643 ± 0.814
<i>ywdA</i>	Hypothetical protein	0.837 ± 0.031	2.119 ± 0.684

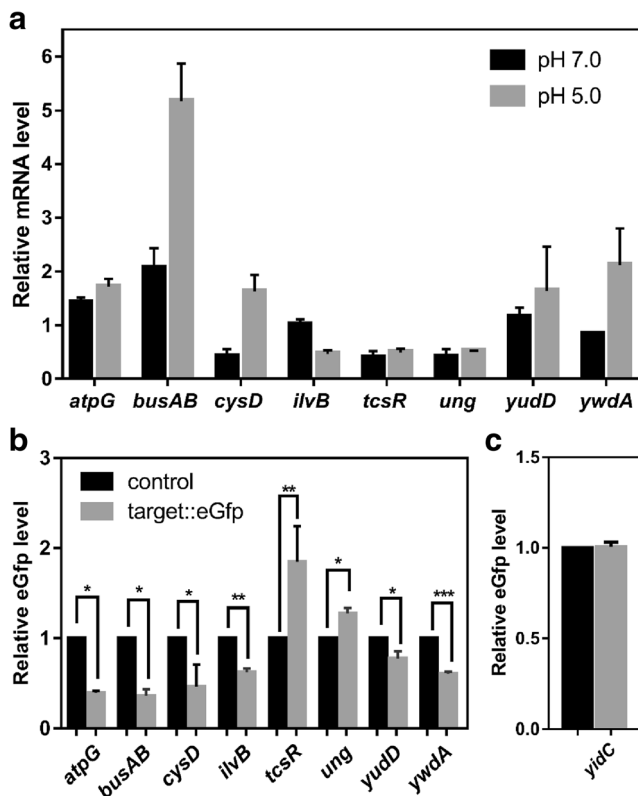


**Fig. 6** **a** mRNA expression levels of candidate genes in *L. lactis* F44- $\Delta$ s015 compared to the wild type at pH 7.0 and 5.0. **b** eGfp levels of candidate genes and **c** a negative control as measured using reporter plasmids. Error bars represent the SD. Statistical differences between each group were analyzed using Student's *t* test; \**p* < 0.05, \*\**p* < 0.005, \*\*\**p* < 0.0005

(Zuker 2003). Four stem-loop structures were predicted, as shown in Fig. 4a. The first stem-loop and the second one are rich of A–U pairs, indicating an unstable region to bind to target mRNAs. Potential targets of s015 were predicted by three software programs: sTarPicker, CopraRNA, and IntaRNA, and Target RNA 2.0; results are shown in Table S3. The target genes identified by each program are summarized in a Venn diagram in Fig. 4b and c. A region located between the first and the second stem-loop structure of s015 was identified as the possible regulatory core. The predicted interaction regions of s015 controlled 74 candidate targets (Fig. 5a–c). Twelve predicted target genes, *atpG*, *busAB*, *cysD*, *ilvB*, *tcsR*, *ung*, *yudD*, *ywdA*, *yrbI*, *ftsW*, *tcsK*, and *SufS*, were selected for further validation.

#### Validation of s015 target genes by qRT-PCR and reporter fusions

To investigate the effect of s015 on 12 target genes, the transcription levels of these target genes in *L. lactis* F44 and F44- $\Delta$ s015 were analyzed by qRT-PCR. As shown in Fig. 6a, at pH 7.0, the mRNA levels of *atpG*, *busAB*, and *yudD* were higher in F44- $\Delta$ s015 compared to F44, while the mRNA levels of *cysD*, *tcsR*, and *ung* were lower. *ilvB* and *ywdA*

mRNA levels displayed little difference between two strains. At pH 5.0, the mRNA levels of *atpG*, *busAB*, *cysD*, *yudD*, and *ywdA* were higher in F44- $\Delta$ s015 compared to F44, while the mRNA levels of *ilvB*, *tcsR*, and *ung* were noticeably lower (as shown in Table 2). But the mRNA level of *yrbI*, *ftsW*, *tcsK*, and *SufS* showed little change in F44- $\Delta$ s015 compared to F44 at both pH 7.0 and pH 5.0 (data not shown). Taken together, these results suggested that s015 is responsible for the inhibition of *atpG*, *busAB*, *cysD*, *yudD*, and *ywdA* as well as upregulation of *ilvB*, *tcsR*, and *ung* at pH 5.0.

To further assess the effect of s015 on its target genes, we designed fusion constructs containing a *lacZ* gene fragment in front of the binding sites of each target gene followed by a green fluorescent protein (GFP) driven by a constitutive promoter. The eGfp levels were then assayed in the presence of either a nonsense sRNA or sRNA s015 after co-transforming along with the target gene::eGfp fusion construct into *E. coli* BL21 (Fig. S1). Compared to the nonsense sRNA, s015 repressed *atpG*::eGfp, *busAB*::eGfp, *cysD*::eGfp, *ilvB*::eGfp, *yudD*::eGfp, and *ywdA*::eGfp by approximately 2.56-fold, 2.50-fold, 2.17-fold, 1.61-fold, 1.61-fold, and 1.67-fold, respectively. In contrast, it increased *tcsR*::eGfp and *ung*::eGfp by 1.85-fold and 1.31-fold, respectively (Fig. 6b). A negative control, *yidC*::eGfp, showed almost no difference in eGfp level between the nonsense control and sRNA s015 (Fig. 6c). Collectively, these results demonstrated that s015 could either inhibit or activate its target genes at the post-transcriptional level.

#### The conserved region of sRNA s015 directly inhibits/activates target gene expression by an antisense mechanism

Bioinformatics analysis suggested that the predicted targets, *atpG*, *busAB*, *cysD*, *ilvB*, *tcsR*, *ung*, *yudD*, and *ywdA*, are direct binding partners of s015 (Fig. 7a–h). To experimentally assess the putative base-pairing interactions, mutations of nucleotides within the predicted interaction regions were introduced. Specifically, s015-mut-1 involved mutations in nucleotides 18–26 (GAAAAAAC → CTTTTTTTG) (Fig. 7b, c, d, e, g, h), and s015-mut-2 involved mutations in nucleotides 99–104 (TATTCC → ATAAGG) (Fig. 7a). Our experiments showed that both mutated sRNAs failed to regulate target mRNAs in the manner of the wild-type s015 (Table 3). We observed the repression decreased moderately in eGFP levels in the strain with s015-mut-1 compared to wild-type s015 for *atpG*::eGfp (~1.19-fold for s015-mut-1 vs. ~2.56-fold for wild-type s015, relative to the nonsense control), *cysD*::eGfp (1.02-fold vs. ~2.17-fold), *ilvB*::eGfp (~1.22-fold vs. ~1.61-fold), and *yudD*::eGfp (~1.16-fold vs. ~1.61-fold). The eGfp level of *tcsR*::eGfp was repressed by 1.25-fold when transformed with s015-mut-1, while it was activated by 1.85-fold when transformed with s015 (Table 3). And *ung*::eGfp was

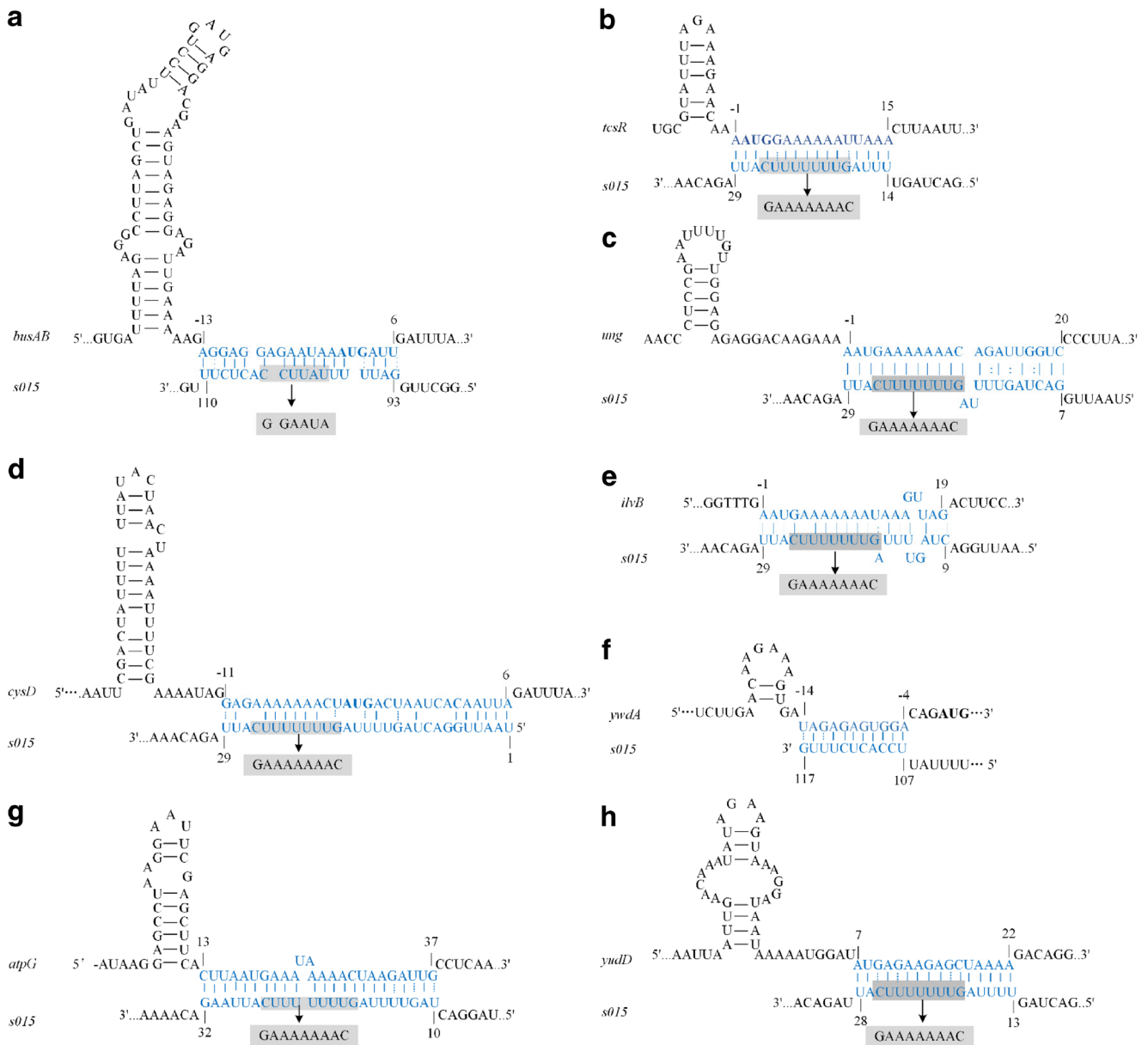


**Fig. 7** Predicted base-pairing interactions between s015 and **a** *busAB*, **b** *tcsR*, **c** *ung*, **d** *cysD*, **e** *ilvB*, **f** *ywdA*, **g** *atpG*, and **h** *yudD* as determined using the CopraRNA program. Mutations introduced in s015 to test these interactions are indicated in gray

activated by 1.74-fold for s015-mut-1 while by 1.28-fold for wild-type s015 relative to the nonsense control. The eGfp level of *ywdA::eGfp* was not significantly different for s015-mut1 compared to the wild-type s015 because the predicted interaction region for this gene was not located in the mutated region (Fig. 8a). Because *busAB* is the only one predicted to bind to s015-mut-2 region, while the other genes are all predicted to bind to the first region, s015-mut-2 was only applied to *busAB*. For s015-mut-2, the eGfp level of *busAB* was repressed ~1.15-fold compared with ~2.50-fold for wild-type sRNA s015 (Fig. 8b). These results verified that s015 regulates many of its targets, *atpG*, *cysD*, *ilvB*, *tcsR*, *ung*, and *yudD*, using the conserved regions we identified.

## Discussion

In this study, we demonstrated that the novel sRNA s015 plays a critical role in the response to acid stress in *L. lactis* and employs an unstable region to regulate target genes involved in multiple pathways. Here, sRNA s015 was identified as a novel trans-encoded sRNA in *L. lactis* F44, and its homologs are conserved in other 11 *L. lactis* strains.

In *L. lactis* F44, it has been shown that nisin yield can be enhanced by improving acid tolerance (Zhang et al. 2016). Here, we showed that s015 was highly transcribed under acid stress. The growth and relative survival in acidic conditions of the F44- $\Delta$ s015, F44-ps015, and F44-cs015 strains compared

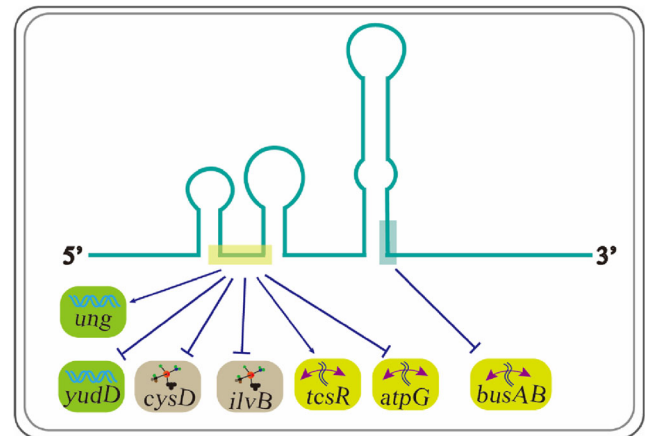


**Table 3** eGFP levels of the fusion reporter relative to the nonsense sRNA control

Target gene	s015	s015-mut
<i>atpG</i>	0.3949 ± 0.0206	0.8454 ± 0.1965
<i>busAB</i>	0.3600 ± 0.0742	0.8709 ± 0.0920
<i>cysD</i>	0.4621 ± 0.2432	0.9801 ± 0.0636
<i>ilvB</i>	0.6201 ± 0.0426	0.8217 ± 0.0592
<i>tcsR</i>	1.8470 ± 0.3929	0.8030 ± 0.0462
<i>ung</i>	1.275 ± 0.0630	1.743 ± 0.2576
<i>yudD</i>	0.6210 ± 0.1301	0.863 ± 0.0823
<i>ywda</i>	0.6084 ± 0.046	0.6027 ± 0.0293
<i>yidC</i>	1.005 ± 0.0256	

to the wild-type *L. lactis* F44 strain indicate that s015 can improve acid tolerance in *L. Lactis* F44. Accordingly, one unit biomass of the s015 overexpression strain *L. lactis* F44-ps015 produced a higher yield of nisin compared to the same biomass of the wild-type F44, F44-*cs015*, and F44- $\Delta$ s015 strains. We could thus infer that s015 enhanced nisin yield by improving the acid tolerance of *L. lactis* F44.

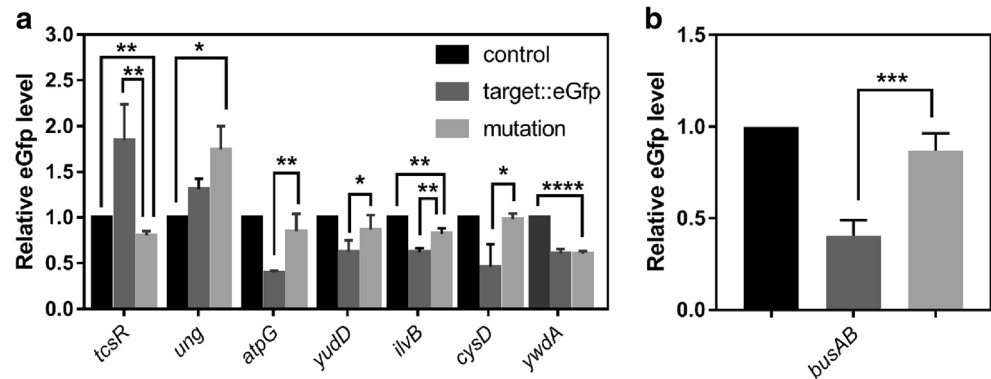
The secondary structure of sRNAs determines their target specificity. Specific regions are responsible for maintaining stability and binding to the RBS and/or coding sequence (CDS) of target mRNAs. Bioinformatics and statistical analysis of predicted s015 target genes revealed that s015 employs a conserved region to interact with individual targets. In *Salmonella*, two conserved regions of SdsR, one located in the distal sequence of the first stem-loop and the other located downstream of an RNaseE-dependent cleavage site in the center of sRNA SdsR molecule, could regulate target genes (Frohlich et al. 2016). In *P. aeruginosa*, sRNA RgsA also possess a conserved region that acts as the regulatory core of the sRNA to inhibit its targets (Lu et al. 2016). In this vein, our work indicated that s015 has a highly conserved single-stranded region (18–26, GAAAAAAAC) that was able to bind to several target mRNAs, as this region is not stable and can easily cross-link with specific target mRNAs, including *atpG*, *cysD*, *ilvB*, *tcsR*, *ung*, *yudD*. In contrast, the gene *ywda* was not predicted to interact at the conserved single-

**Fig. 9** s015 employs a conserved target site (light yellow box) to regulate six target mRNAs identified in this study, s015 cross-links with mRNA busAB on the light blue region

stranded region, and accordingly, we showed that the s015-mut-1 effected no change in eGfp levels compared to the wild-type s015. From our data, we inferred that the region of s015 encompassing nucleotides 18–26 (GAAAAAAAC) is the interaction region responsible for the regulation of many specific target genes (Fig. 9).

Targeting deeper into the CDS (i.e., downstream of the first five codons in an area where mRNAs are generally sensitive to antisense inhibition of translation initiation) has been reported as a common mechanism of sRNA-mediated regulation (Frohlich et al. 2012). In this work, the region of s015 encompassing nucleotides 10–32 was shown to bind to the deeper CDS (codons 5–13) of *atpG*, and the eGfp validation experiment showed that *atpG* was repressed by s015. These results suggested that s015 might repress the expression of *atpG* through the translation blockage as occurs in *P. aeruginosa* with regulation of *fis* by the sRNA RgsA (Lu et al. 2016).

Base-pairing between an sRNA and its target mRNA usually leads to mRNA degradation, repression of translation, or both (Storz et al. 2011; Waters and Storz 2009). A wealth of sRNAs bind to the RBS of their target genes to repress translation and decrease mRNA levels. For example, in *P. aeruginosa*, RgsA interacts with a region within the *acpP* RBS to form a “kissing

**Fig. 8** s015-target mRNA interactions were validated by mutating the predicted target gene interaction sites in s015 sRNA. s015 was mutated to **a** s015-mut-1 or **b** s015-mut-2. Statistical differences between each group were analyzed using Student's *t* test; \**p* < 0.05, \*\**p* < 0.005, \*\*\**p* < 0.0005

complex” (Lu et al. 2016). Here, we found that *s015* could bind around the RBS of *busAB*, *cysD*, and *ywdA*, leading to the repression of transcript levels through translational inhibition. In *Enterobacteria*, the MicC sRNA binds to the coding sequence of the *ompD* mRNA and directly promotes its degradation (Pfeiffer et al. 2009). Here, *yudD* mRNA was degraded due to secondary structure changes induced by binding of *s015*. The 5' UTR of target mRNAs may fold into a hairpin that sequesters the RBS into a double-stranded secondary structure, inhibiting translation initiation. The sRNAs *RprA*, *DsrA*, and *ArcZ* can bind to a specific site within the *rpoS* 5' UTR and sequester sequences that would otherwise participate in forming the translation-inhibitory structure, thereby relieving translational inhibition (Mika and Hengge 2014; Soper and Woodson 2008). In a similar vein, our data suggested that *s015* could relieve the RBS blocks of *tsrR* and *ung* mRNAs by binding to the base-pair sequence that formed a double-stranded hairpin. For *ilvB*, validation by qRT-PCR and reporter plasmids yielded conflicting results. Further study indicated that a possible binding site of *ilvB* was located upstream of the start codon. This might indicate the competition between the two binding targets and needs to be investigated further.

Located in intergenic regions and shown to act on targets elsewhere in the genome, trans-encoded sRNAs control multiple target mRNAs via imperfect base-pairing, and there is evidence that this mechanism is prominent in bacteria (Boisset et al. 2007; Chunhua et al. 2012). The sRNA *s015* is present in the intergenic region between two ORFs, as is shown in Fig. S3. Due to the distance between *s015* and its flanking ORFs, it is likely that it does not interact directly with these ORFs; rather, it is more plausible that its targets are located elsewhere in the genome.

To summarize, as a non-coding regulator, *s015* assisted *L. lactis* F44 in surviving acidic conditions. Although not all predicted *s015* target candidates were validated in this work, we have identified several target genes (*atpG*, *busAB*, *cysD*, *ilvB*, *tsrR*, *ung*, *yudD*, and *ywdA*) and characterized their interactions with *s015*. Taken together, our data indicate that the sRNA *s015* has vital roles in regulating genes involved in responding to acid stress. Our study could assist us better understand how *L. lactis* responds to various environmental stress conditions. These findings also enhance our knowledge of the mechanisms that *s015* directly inhibit or activate target mRNAs.

**Acknowledgments** This project was financially supported by the National Key Technology Support Program (2015BAD16B04), the National Natural Science Foundation of China (31570049, 32570089), and the Funds for Creative Research Groups of China (21621004). J.Q. was supported by The New Century Outstanding Talent Support Program, Education Ministry of China.

#### Compliance with ethical standards

**Competing financial interests** The authors declare no competing financial interests.

**Ethical approval** This work does not include any studies with human participants or animals.

## References

- Bak G, Han K, Kim D, Lee Y (2014) Roles of rpoS-activating small RNAs in pathways leading to acid resistance of *Escherichia coli*. *Microbiology* 3:15–28. doi:10.1002/mbo3.143
- Bardill JP, Zhao X, Hammer BK (2011) The *Vibrio cholerae* quorum sensing response is mediated by Hfq-dependent sRNA/mRNA base pairing interactions. *Mol Microbiol* 80:1381–1394. doi:10.1111/j.1365-2958.2011.07655.x
- Boisset S, Geissmann T, Huntzinger E, Fechter P, Bendridi N, Possedko M, Chevalier C, Helfer AC, Benito Y, Jacquier A, Gaspin C, Vandenesch F, Romby P (2007) *Staphylococcus aureus* RNAIII coordinately represses the synthesis of virulence factors and the transcription regulator rot by an antisense mechanism. *Genes Dev* 21:1353–1366. doi:10.1101/gad.423507
- Busch A, Richter AS, Backofen R (2008) IntaRNA: efficient prediction of bacterial sRNA targets incorporating target site accessibility and seed regions. *Bioinformatics* 24:2849–2856. doi:10.1093/bioinformatics/btn544
- Chunhua M, Yu L, Yaping G, Jie D, Qiang L, Xiaorong T, Guang Y (2012) The expression of LytM is down-regulated by RNAIII in *Staphylococcus aureus*. *J Basic Microbiol* 52:636–641. doi:10.1002/jobm.201100426
- Frohlich KS, Haneke K, Papenfort K, Vogel J (2016) The target spectrum of SdsR small RNA in *Salmonella*. *Nucleic Acids Res*. doi:10.1093/nar/gkw632
- Frohlich KS, Papenfort K, Berger AA, Vogel J (2012) A conserved RpoS-dependent small RNA controls the synthesis of major porin OmpD. *Nucleic Acids Res* 40:3623–3640. doi:10.1093/nar/gkr1156
- Huntzinger E, Boisset S, Saveanu C, Benito Y, Geissmann T, Namane A, Lina G, Etienne J, Ehresmann B, Ehresmann C, Jacquier A, Vandenesch F, Romby P (2005) *Staphylococcus aureus* RNAIII and the endoribonuclease III coordinately regulate spa gene expression. *EMBO J* 24:824–835. doi:10.1038/sj.emboj.7600572
- Kery MB, Feldman M, Livny J, Tjaden B (2014) TargetRNA2: identifying targets of small regulatory RNAs in bacteria. *Nucleic Acids Res* 42:W124–W129. doi:10.1093/nar/gku317
- Klahn S, Schaal C, Georg J, Baumgartner D, Knippen G, Hagemann M, Muro-Pastor AM, Hess WR (2015) The sRNA NsiR4 is involved in nitrogen assimilation control in cyanobacteria by targeting glutamine synthetase inactivating factor IF7. *Proc Natl Acad Sci U S A* 112:E6243–E6252. doi:10.1073/pnas.1508412112
- Lu P, Wang Y, Zhang Y, Hu Y, Thompson KM, Chen S (2016) RpoS-dependent sRNA RgsA regulates Fis and AcpP in *Pseudomonas aeruginosa*. *Mol Microbiol* 102:244–259. doi:10.1111/mmi.13458
- Mika F, Hengge R (2014) Small RNAs in the control of RpoS, CsgD, and biofilm architecture of *Escherichia coli*. *RNA Biol* 11:494–507. doi:10.4161/rna.28867
- Morfeldt E, Taylor D, von Gabain A, Arvidson S (1995) Activation of alpha-toxin translation in *Staphylococcus aureus* by the trans-encoded antisense RNA, RNAIII. *EMBO J* 14:4569–4577
- Opdyke JA, Kang JG, Storz G (2004) GadY, a small-RNA regulator of acid response genes in *Escherichia coli*. *J Bacteriol* 186:6698–6705. doi:10.1128/jb.186.20.6698-6705.2004
- Pain A, Ott A, Amine H, Rochat T, Boulou P, Gautheret D (2015) An assessment of bacterial small RNA target prediction programs. *RNA Biol* 12:509–513. doi:10.1080/15476286.2015.1020269
- Pfeiffer V, Papenfort K, Lucchini S, Hinton JC, Vogel J (2009) Coding sequence targeting by MicC RNA reveals bacterial mRNA silencing

- downstream of translational initiation. *Nat Struct Mol Biol* 16:840–846. doi:10.1038/nsmb.1631
- Rayman MK, Aris B, Hurst A (1981) Nisin: a possible alternative or adjunct to nitrite in the preservation of meats. *Appl Environ Microbiol* 41:375–380
- Romeo Y, Bouvier J, Gutierrez C (2007) Osmotic regulation of transcription in *Lactococcus lactis*: ionic strength-dependent binding of the BusR repressor to the busA promoter. *FEBS Lett* 581:3387–3390. doi:10.1016/j.febslet.2007.06.037
- Siqueira FM, de Morais GL, Higashi S, Beier LS, Breyer GM, de Sa Godinho CP, Sagot MF, Schrank IS, Zaha A, de Vasconcelos AT (2016) Mycoplasma non-coding RNA: identification of small RNAs and targets. *BMC Genomics* 17:743. doi:10.1186/s12864-016-3061-z
- Soper TJ, Woodson SA (2008) The *rhoS* mRNA leader recruits Hfq to facilitate annealing with DsrA sRNA. *RNA* 14:1907–1917. doi:10.1261/rna.1110608
- Stevens KA, Sheldon BW, Klapes NA, Klaenhammer TR (1991) Nisin treatment for inactivation of *Salmonella* species and other gram-negative bacteria. *Appl Environ Microbiol* 57:3613–3615
- Storz G, Vogel J, Wassarman KM (2011) Regulation by small RNAs in bacteria: expanding frontiers. *Mol Cell* 43:880–891. doi:10.1016/j.molcel.2011.08.022
- Updegrave TB, Shabalina SA, Storz G (2015) How do base-pairing small RNAs evolve? *FEMS Microbiol Rev* 39:379–391. doi:10.1093/femsre/fuv014
- Urban JH, Vogel J (2007) Translational control and target recognition by *Escherichia coli* small RNAs in vivo. *Nucleic Acids Res* 35:1018–1037. doi:10.1093/nar/gkl1040
- van der Meulen SB, de Jong A, Kok J (2016) Transcriptome landscape of *Lactococcus lactis* reveals many novel RNAs including a small regulatory RNA involved in carbon uptake and metabolism. *RNA Biol* 13:353–366. doi:10.1080/15476286.2016.1146855
- Wagner EG, Romby P (2015) Small RNAs in bacteria and archaea: who they are, what they do, and how they do it. *Adv Genet* 90:133–208. doi:10.1016/bs.adgen.2015.05.001
- Wang J, Liu T, Zhao B, Lu Q, Wang Z, Cao Y, Li W (2016a) sRNATarBase 3.0: an updated database for sRNA-target interactions in bacteria. *Nucleic Acids Res* 44:D248–D253. doi:10.1093/nar/gkv1127
- Wang L, Wang W, Li F, Zhang J, Wu J, Gong Q, Shi Y (2015) Structural insights into the recognition of the internal A-rich linker from OxyS sRNA by *Escherichia coli* Hfq. *Nucleic Acids Res* 43:2400–2411. doi:10.1093/nar/gkv072
- Wang L, Yang G, Qi L, Li X, Jia L, Xie J, Qiu S, Li P, Hao R, Wu Z, Du X, Li W, Song H (2016b) A novel small RNA regulates tolerance and virulence in *Shigella flexneri* by responding to acidic environmental changes. *Front Cell Infect Microbiol* 6:24. doi:10.3389/fcimb.2016.00024
- Waters LS, Storz G (2009) Regulatory RNAs in bacteria. *Cell* 136:615–628. doi:10.1016/j.cell.2009.01.043
- Waugh A, Gendron P, Altman R, Brown JW, Case D, Gautheret D, Harvey SC, Leontis N, Westbrook J, Westhof E, Zuker M, Major F (2002) RNAML: a standard syntax for exchanging RNA information. *RNA* 8:707–717
- Wenner N, Maes A, Cotado-Sampayo M, Lapouge K (2014) NrsZ: a novel, processed, nitrogen-dependent, small non-coding RNA that regulates *Pseudomonas aeruginosa* PAO1 virulence. *Environ Microbiol* 16:1053–1068. doi:10.1111/1462-2920.12272
- Wright PR, Georg J, Mann M, Sorescu DA, Richter AS, Lott S, Kleinkauf R, Hess WR, Backofen R (2014) CopraRNA and IntaRNA: predicting small RNA targets, networks and interaction domains. *Nucleic Acids Res* 42:W119–W123. doi:10.1093/nar/gku359
- Xuanyuan Z, Wu Z, Li R, Jiang D, Su J, Xu H, Bai Y, Zhang X, Saris PE, Qiao M (2010) Loss of IrpT function in *Lactococcus lactis* subsp. *lactis* N8 results in increased nisin resistance. *Curr Microbiol* 61:329–334. doi:10.1007/s00284-010-9615-4
- Zere TR, Vakulskas CA, Leng Y, Pannuri A, Potts AH, Dias R, Tang D, Kolaczowski B, Georgellis D, Ahmer BM, Romeo T (2015) Genomic targets and features of BarA-UvrY (–SirA) signal transduction systems. *PLoS One* 10:e0145035. doi:10.1371/journal.pone.0145035
- Zhang J, Caiyin Q, Feng W, Zhao X, Qiao B, Zhao G, Qiao J (2016) Enhance nisin yield via improving acid-tolerant capability of *Lactococcus lactis* F44. *Sci Rep* 6:27973. doi:10.1038/srep27973
- Zhang YF, Liu SY, Du YH, Feng WJ, Liu JH, Qiao JJ (2014) Genome shuffling of *Lactococcus lactis* subspecies *lactis* YF11 for improving nisin Z production and comparative analysis. *J Dairy Sci* 97:2528–2541. doi:10.3168/jds.2013-7238
- Zhu D, Zhao K, Xu H, Zhang X, Bai Y, Saris PEJ, Qiao M (2014) Construction of *thyA* deficient *Lactococcus lactis* using the Cre-loxP recombination system. *Ann Microbiol* 65:1659–1665. doi:10.1007/s13213-014-1005-x
- Zuker M (2003) Mfold web server for nucleic acid folding and hybridization prediction. *Nucleic Acids Res* 31:3406–3415
- Zuker M, Jacobson AB (1998) Using reliability information to annotate RNA secondary structures. *RNA* 4:669–679